Heliyon 10 (2024) e30169

Contents lists available at ScienceDirect

Heliyon

journal homepage: www.cell.com/heliyon

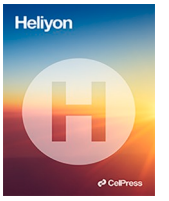

Research article

Strictosamide promotes wound healing through activation of the PI3K/AKT pathway

Gu-xu Ming [a], Jun-yan Liu [a], Yu-huang Wu [a], Li-yan Li [a], Xin-yue Ma [a], Pei Liu [b], Yi-peng Pan [b,*], Xiao-ning He [b,**], Yong-hui Li [a,b,***]

[a] *Hainan Provincial Key Laboratory R&D on Tropical Herbs, Haikou Key Laboratory of Li Nationality Medicine, School of Pharmacy, Hainan Medical University, Haikou, China*
[b] *The Second Affiliated Hospital, Hainan Medical University, Haikou, China*

ARTICLE INFO

Keywords:
Strictosamide
Wound healing
Network pharmacology
Molecular docking
PI3K/AKT pathway
Validation *in vivo and in vitro*

ABSTRACT

Nauclea officinalis, as a Chinese medicine in Hainan province, had the effect of treating lower limb ulcers, burn infections. In this paper, we studied the effect of Strictosamide (STR), the main bioactive compound in *Nauclea officinals*, on wound healing and explored its internal mechanism. Firstly, the wound healing potential of STR was evaluated in a rat model, demonstrating its ability to expedite wound healing, mitigate inflammatory infiltration, and enhance collagen deposition. Additionally, immunofluorescence analysis revealed that STR up-regulated the expression of CD31 and PCNA. Subsequently, target prediction, protein-protein interaction (PPI), gene ontology (GO), and pathway enrichment analyses were used to obtain potential targets, specific biological processes, and molecular mechanisms of STR for the potential treatment of wound healing. Furthermore, molecular docking was conducted to predict the binding affinity between STR and its associated targets. Additionally, *in vivo* and *in vitro* experiments confirmed that STR could increase the expression of P-PI3K, P-AKT and P-mTOR by activating the PI3K/AKT signaling pathway. In summary, this study provided a new explanation for the mechanism by which STR promotes wound healing through network pharmacology, suggesting that STR may be a new candidate for treating wound.

1. Introduction

Skin was the human body's barrier against external infection and plays an important role in protecting the organism from mechanical and chemical injury or pathogens invasion [1]. Wound was a common disease on routine life with a high incidence, if not treated, will result to severe infection, even death [2]. At present, the mainstream drugs for wound healing in clinical practice were cell growth factors, including platelet-derived growth factors, basic fibroblast growth factors and granulocyte-macrophage colony-stimulating factors [3]. However, due to their high treatment expenditure and special storage conditions, there were many invariants for the usage of these drugs. Therefore, finding new drugs to promote wound healing had always been the focus of drug discovery.

* Corresponding author.
** Corresponding author.
*** Corresponding author. Hainan Provincial Key Laboratory R&D on Tropical Herbs, Haikou Key Laboratory of Li Nationality Medicine, School of Pharmacy, Hainan Medical University, Haikou, China.
E-mail addresses: 641795334@qq.com (Y.-p. Pan), hexiaoningvv@aliyun.com (X.-n. He), lyhssl@126.com (Y.-h. Li).

https://doi.org/10.1016/j.heliyon.2024.e30169
Received 12 May 2023; Received in revised form 19 April 2024; Accepted 22 April 2024
Available online 23 April 2024

List of abbreviations

STR	Strictosamide
PCNA	Proliferating cell nuclear antigen
PECAM-1	Platelet endothelial cell adhesion molecule-1
LPS	Lipopolysaccharides
HUVEC	Human umbilical vein endothelial cells
H&E	Hematoxylin and eosin
SD	Sprague Dawley
BP	Biological process
MF	Molecular function
CC	Cellular component
ANOVA	One-way analysis of variance

In clinical practice, wound healing consist four continuous and overlapping phases: homeostasis, inflammation, proliferation, and tissue remodeling [4]. The proliferation period was the primary period for wound healing. During this phase, fibroblasts proliferate and collagen was deposited. Concurrently, vascular endothelial cells assemble to form micro vascular structures [5]. Fibroblast proliferation, collagen deposition and angiogenesis were the important processes for wound healing [6]. CD31 known as platelet endothelial cell adhesion molecule-1 (PECAM-1), was regarded as a marker of peripheral vessel endothelial cell [7]. Increased expression of CD31 in the healing tissue indicates more angiogenesis. Proliferating cell nuclear antigen (PCNA) was a nuclear protein existed in all eukaryotic species, which takes part in DNA synthesis and repair process, cell proliferation and cell cycle [8]. The expression level of PCNA could reflect the degree of cell proliferation [9].

The plants of *Nauclea* mainly distributed in tropical regions, and their main chemical components were alkaloids. *Nauclea* plants had various pharmacological activities and had been traditionally used to treat cold, fever, inflammation, pain relief and ulcer [10]. *Nauclea officinalis* Pierre ex Pitard, a plant of Nauclea genus, had remarkable therapeutic effects against various infectious diseases among Chinese people [11]. Danmu extract syrup and Danmu extract tablet were two Chinese patent drugs made by *Nauclea officinalis*, had been used to treat colds, fever, and various viral inflammations in clinical practice [12]. And previous clinical study had also demonstrated that Danmu extract tablets could effectively treat cystic acne [13]. After treated with Danmu extract tablets for 4 weeks, acne cysts were significantly reduced, and the overall effective rate could reach 78 %.

Strictosamide (STR), the main chemical component of *Nauclea* genus [14–16], had attracted the attention of researchers due to its diverse pharmacological activities, including proliferation [17], anti-inflammatory effects [18], and antibacterial activities [19]. Study on anti-inflammatory mechanisms had shown that STR could reduce the NO, TNF-α and IL-1β in lipopolysaccharides (LPS)-induced RAW 264.7 cells [18]. Our previous research also found STR could promote the proliferation of human umbilical vein endothelial cells (HUVEC) and up-regulate the expression level of VEGF in HUVECs [20]. However, the bioactivity and the mechanism of STR on wound healing had not been reported.

Network pharmacology was a new developed technique, and had shown a promising prospect in predicting the mechanism of action of compounds in the treatment of complex diseases [21]. Through multiple computer software and databases, such as Cytoscape 3.9.1 and Gene Cards, it interprets the potential targets and mechanism of drug therapy for diseases in a multidirectional manner [22]. By network pharmacology, Tang successfully predicted that *Morusalba* could alleviate diabetes mellitus through TNF signaling pathway and NF-κB signaling [23]. And it was very suitable for predicting the mechanism of action of compounds [24].

In this paper, we firstly reported the promoting effect of STR on wound healing. And also for the first time, network pharmacology was applied to predict and verify the mechanism of action of STR. The results showed that STR could promote cell repair and wound healing by regulating PI3K/AKT/mTOR. These results will promote the application of STR in wound healing. Fig. 1 represented a schematic diagram of the present study.

2. Data and methods

2.1. Drugs and materials

STR(CAS NO.: 23141-25-5, HPLC purity ≥99 %) was purchased from Shanghai Macklin Biochemical Technology Co., Ltd. The chemical structure of STR was shown in Fig. 2. The primary antibodies including anti-CD31 and anti-PCNA were purchased from Abcam. The primary antibodies including anti-PI3K, anti-P-PI3K, anti-AKT, anti-P-AKT, anti-mTOR and anti-P-mTOR were purchased from Cell Signaling Technology. Recombinant bovine basic fibroblast growth factor gel (rb-bfgf) obtained from Zhuhai Yisheng Biopharmaceutical Co. LTD (GuangZhou, China, lot number: 04220403).

2.2. Cell culture

NCTC clone 929 (L929) fibroblast and Human Umbilical Vein Endothelial Cells (HUVEC) were purchased from Newgain Biopharmaceutical Co., LTD (Wu Xi, China). The cells were cultured in DMEM complete medium containing 10 % fetal bovine serum

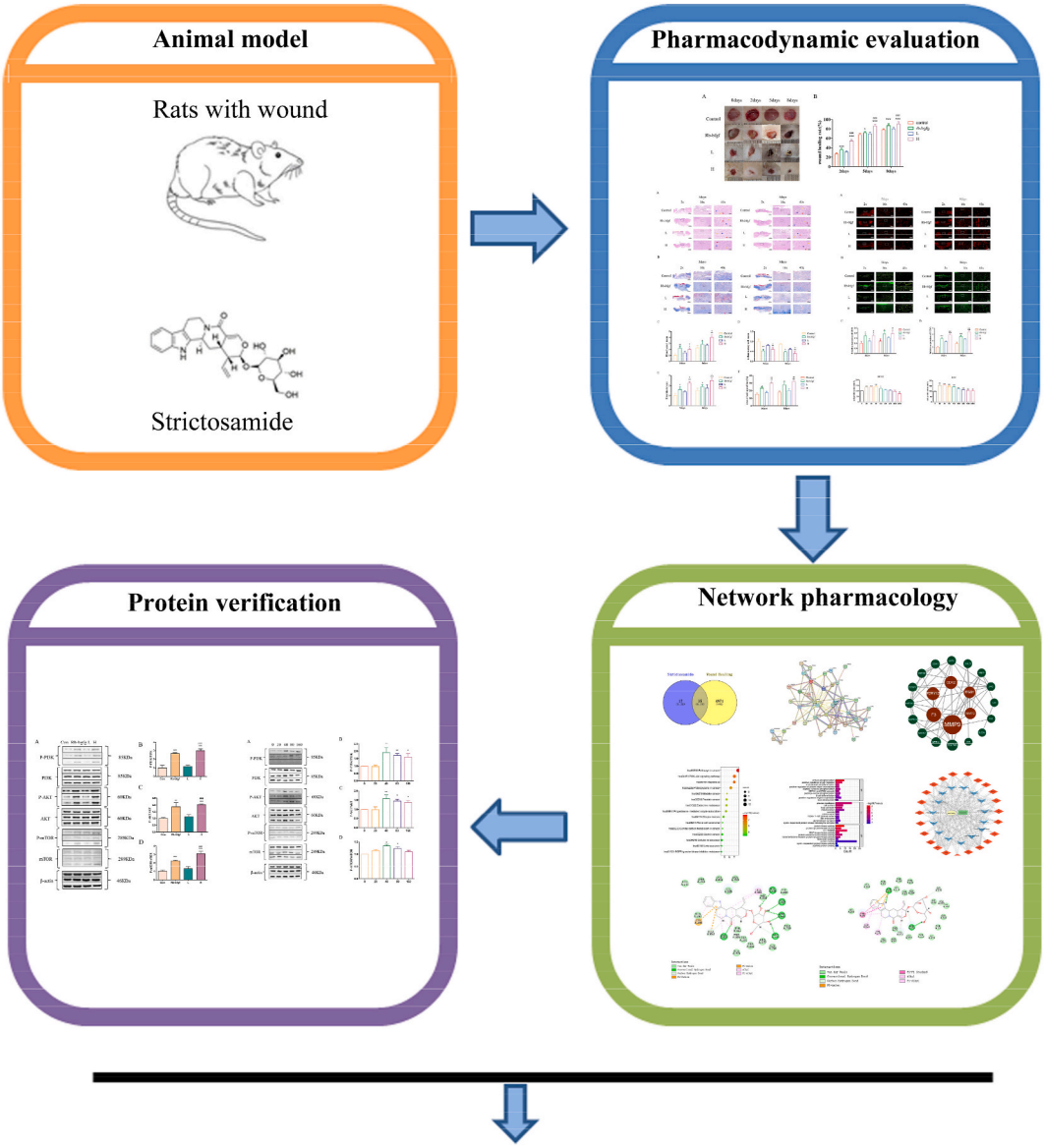

Fig. 1. The graphical abstract of the present study.

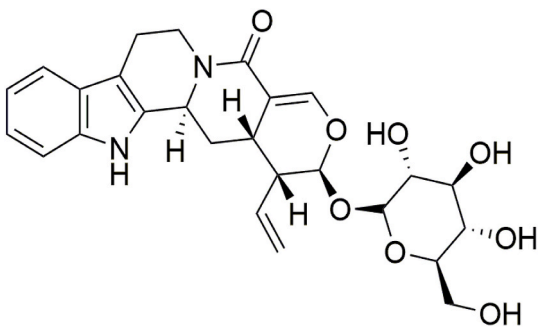

Fig. 2. The chemical structure of STR.

(Gibco, USA), 100U/mL penicillin and 100 μg/mL streptomycin (Corning, USA). The cells were maintained at 37 °C and 5 % CO_2 in a CO_2 incubator.

2.3. Animals

Forty-eight male Sprague Dawley (SD) rats (200–220 g), were obtained from Changsha Tianqin Biotechnology Co., LTD (Hunan, China, Certificate No. SCXK-2022-0011). All rats were housed in a specific-pathogen free environment at 22 ± 2 °C with 55 ± 2 % humidity and a 12 h light/12 h dark cycle. All rats had free access to food and water. All animal experiment procedures were approved by the Animal Ethical Committee of Hainan Medical University (approval No. HYLL-2022-277).

2.4. Animal experimental design

A tissue biopsy instrument with a diameter of 8 mm was used to remove full-thickness skin on the back of the rats [25]. The day of the wound formation was marked as day 0. After the wound model was established, the rats were divided into four groups randomly (n = 12): control group (normal saline); rb-bfgf group (2122IU/kg, rb-bfgf gel); L group (0.5 mg/kg, STR); H group (1.5 mg/kg, STR), respectively. STR was completely dissolved in normal saline and the concentration was 7.5 mM. The rats were raised in separated cages and sterile gauze containing drugs was applied for treatment from day 1 to day 8 with a dose of 100 μL twice a day. The dosage of each group of rats was referred to the published literature and the actual solubility [26]. The photographs of the wound were taken at the same angle and height. The measurements of wound area were taken on the days 0, 2, 5 and 8. The area of the wound was calculated by Image J software. Wound healing rate was taken the initial (day 0) size of the wound as 100 %. The calculation formula of wound healing rate was as follows: wound healing rate $(\%) = \frac{\text{wound area on day 0-wound area on day N}}{\text{wound area on day 0}} * 100$ (N = 0, 2, 5, 8).

On the days 5 and 8 after wound modeling, the rats were euthanized by neck dislocation and full-thickness skin including wound and the 3 mm of skin around the wound were collected [6]. The tissues were divided into two parts. The first part was stored in 4 % paraformaldehyde solution for histological analysis and immunohistochemistry. The second part was used to perform Western blot for the analysis of target proteins. Fig. 3 showed the flow graph of the experimental process.

2.5. Histological analysis

On day 5 and 8 post-wounding, the wound tissues were excised and fixed in 4 % paraformaldehyde solution for 36 h. After being routinely processed by standard procedures, a series of 3 μm sections were obtained by paraffin microtome. Next, the sections were subjected to hematoxylin and eosin staining (H&E) and Masson staining respectively. The images were captured using the software of CaseViewer Native Windows Application. Six fields (3 fields in the dermis - upper cortex and 3 fields in the dermis - lower cortex) of each section of the four groups of rats were analyzed under a 400 × magnifying glass to detect inflammatory infiltration and fibroplasia. Visual field images with 100 × magnification in the cuticle dermo subcutaneous direction were evaluated to quantify angiogenesis. The Image J software "Cell Counter" plugin at 400 × magnification was used to count inflammatory infiltrates, blood vessels and fibroblasts [27].

2.6. Immunofluorescence analysis

In order to observe the proliferation and angiogenesis during wound healing, the immunofluorescence was conducted to detect the expression of PCNA and CD31 antigens respectively. The tissue sections were washed with PBS, blocked with 0.25 % Triton 100 and 6 % BSA, and incubated with anti-PCNA (ab29, 1:1000) or anti-CD31 (ab182981, 1:2000) at 4 °C. Then, the tissue sections were washed and further incubated with Alexa Fluor ® 647 (1:500, ab150083) for 1 h. Subsequently, the cell nuclei were stained with 4, 6-diamidino-2-phenylindole (Cell Signaling Technology, Shanghai, China).

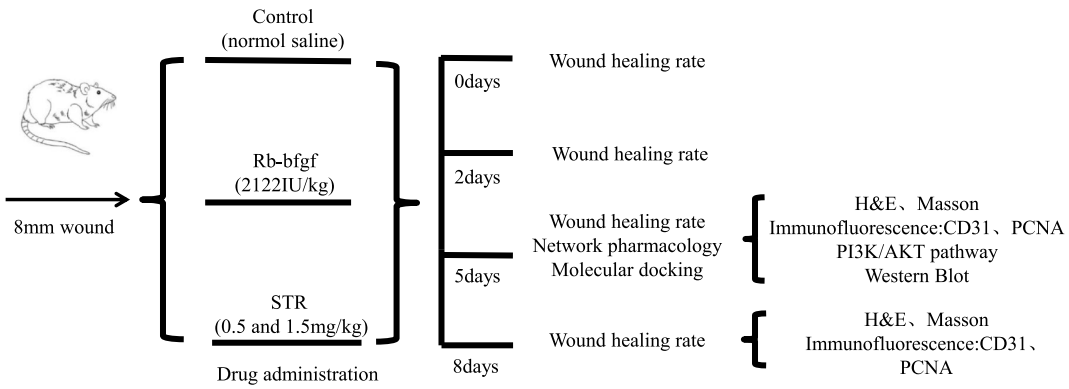

Fig. 3. Flow graph of the experimental process.

2.7. Network pharmacology analysis

2.7.1. STR and wound healing-related gene analysis

The 2D structure of STR was obtained from the PubChem database (https://pubchem.ncbi.nlm.nih.gov/) [28] and was entered into Swiss-Target-Prediction database (http://www.swisstargetprediction.ch/) to predict STR-related targets. The targets with probability >0 were selected for further investigation.

The DisGeNET database (https://www.disgenet.org) was searched with the keyword "wound healing" to screen wound healing-related genes and screened based on a score >0. The intersected genes were obtained using Venny 2.1.0 (https://bioinfogp.cnb.csic.es/tools/venny/index.html).

2.7.2. Hub node screening

The intersected targets STR and wound healing were imported into the String database (http://string-db.org/). Then, the protein interaction network diagram obtained. After downloading the diagram, it was imported to cytoscape 3.9.1 to obtain Intermediate number centrality. The hub nodes were screened according to the degree of intermediate number centrality.

2.7.3. Hub node GO and KEGG enrichment analysis

The GO terms of biological process (BP), molecular function (MF), and cellular component (CC) and signaling pathways were analyzed using the R package cluster profiler for GO and KEGG enrichment analysis of hub nodes. The top 15 BP, MF and CC, and important KEGG pathways were screened according to the corrected P-value <0.05.

2.7.4. Compound-target-pathway-disease network construction

The information of STR, wound healing, active targets, and related pathways were imported into Cytoscape 3.9.1 software to construct a compound-target-pathway-disease network [29]. The nodes in the network represent STR, targets, pathways, and wound healing, and the connecting lines represent the interactions between the nodes. The importance of the nodes in the network was judged by the topological parameter degree. A higher degree indicated higher node importance in the network since more nodes were directly related to the node in the network.

2.8. Molecular docking

The structure of STR was imported into Discovery Studio 2019. The RCSB database (http://www.RCSB.org) was used to download the crystal structures of AKT (PDB ID: 6HHI) and PI3K (PDB ID: 6AUD). These downloaded protein structures were imported into Discovery Studio 2019. After removing the water molecules and ligands from the structure, the binding site of the protein and STR was determined. Discovery Studio2019 was used to analyze the binding between STR and proteins. And the docking sites and binding energy were recorded.

2.9. CCK-8 assay

The effects of STR on the proliferation of L929 and HUVECs were determined by Cell Counting Kit-8 (CCK-8) (Beyotime, Shanghai, China). The plates were seeded at a density of 2000 cells per well and cultured in a complete culture medium for 24 h. Then, L929 cells and HUVECs were cultured with STR at concentration of 0, 20, 40, 80,160, 320, 625, 1250 and 2500 μM for 24 h were used for CCK-8 assay. Cells were treated with CCK-8 reagent and cultured in the incubator for 2 h. The absorbance value was determined at 450 nm.

2.10. Western blot

According previous research, the 5-day tissues were chosen for the Western blot analysis [6]. Proteins from wound tissues and L929 cells were first extracted by RIPA Lysis Buffer (Boster Biotechnology, Wuhan, China) containing protease inhibitor (Boster Biotechnology, Wuhan, China), and the protein was quantified by BCA protein assay Kit (Boster Biotechnology, Wuhan, China). The proteins were separated by 6 % or 10 % sodium dodecyl sulfate-polyacrylamide gel and then transferred onto polyvinylidenedifluoride membranes. The membranes were blocked with 5 % skim milk for 1 h and then incubated with different primary antibodies: PI3K, P-PI3K (Tyr458/Tyr199), AKT, P-AKT (Ser473), mTOR, P-mTOR and β-actin at 4 °C overnight. After washed with Tris-buffered saline containing Tween 20, the membrane was incubated with the HRP labeled secondary antibody (Proteintech, Chicago, IL, United States) for 1 h at room temperature. Finally, the membrane surface was uniformly coated with the ECL chemiluminescent substrate reagent (Biosharp) and then exposed to the Image Lab analysis system (Bio-Rad, ChemiDocXRS+, United States).

2.11. Statistical analysis

With regard to data analysis, all results were calculated using the GraphPad Prism 7.0. The statistical analysis was done by one-way analysis of variance (ANOVA) followed by Dunnett's test. $P < 0.05$ was considered to be statistically significant.

3. Results

3.1. Effects of STR on wound healing

The therapeutic effects of STR on rat skin wounds were observed on day 2, 5 and 8. As shown in Fig. 4A and B, Rb-bfgf group and H-STR group had better therapeutic effects than the control group on the wound. On day 2, compared with control group, the L-STR group almost had no difference. The wound healing rate of the rb-bfgf group was 35.72 % ± 3.70 % and the H-STR group was 54.42 ± 2.71 %, significantly higher than the control group (26.52 % ± 2.71 %) ($P < 0.05$) and L-STR group (30.72 % ± 2.53 %) ($P < 0.05$). On day 5, the wound healing rates of the control group and the L-STR group were 67.25 % ± 2.89 % and 69.35 ± 3.36 %, respectively. The wound healing rates of the rb-bfgf group and H-STR groups were 71.23 % ± 2.68 % and 79.78 % ± 3.21 %. On day 8, the wound healing rate in the rb-bfgf group and H-STR group were 87.03 % ± 3.84 % and 90.51 % ± 4.92 %, while the control group (77.83 % ± 2.92 %) and the L-STR group (80.65 % ± 3.21 %). Compared with group L, group H had better therapeutic effect. Thus, STR could promote wound healing in general and have concentration dependence.

3.2. Histopathological analysis

As illustrated in Fig. 5A, H&E staining exhibited higher granulation tissue thickness, fewer inflammatory cells infiltration, increased angiogenesis, and increased fibroblast numbers in the H-STR group on both day 5 and day 8. The result obtained by quantitative analysis with image J clearly shows that both the H-STR group and rb-bfgf group had fewer inflammatory cells as well as more blood vessels and fibroblast compared with the control group. On day 5, the relative number of blood vessels of the rb-bfgf group was 211.76 % ± 17.65 % ($P < 0.01$) and the H-STR group was 194.12 % ± 23.34 % ($P < 0.05$), significantly higher than the control group (100 % ± 20.38 %) and L-STR group (141.18 % ± 17.65 %) (Fig. 5C). The relative number of inflammatory cells of the control group and the L-STR group were 100.00 % ± 3.47 % and 75.61 % ± 4.53 %, respectively. The relative number of inflammatory cells of the rb-bfgf group and H-STR groups were 50.68 % ± 5.24 % ($P < 0.01$) and 58.54 % ± 6.07 % ($P < 0.01$). (Fig. 5D). The number of fibroblasts in the rb-bfgf group and H-STR group increased to 170.62 % ± 16.29 % ($P < 0.05$) and 245.76 % ± 9.77 % ($P < 0.01$), compared with the control group (100.00 % ± 11.46 %) and the L-STR group (80.65 % ± 3.21 %) (Fig. 5E). In addition, the number of blood vessels and fibroblasts increased, while inflammatory cells decreased in each group on day 8 compared to day 5.

Collagen was a critical component for tissue regeneration. During the wound healing process, a dramatical and robust increase in the deposition of collagen fibers was observed in wound managed with H-STR and rb-bfgf by mason's trichrome staining (Fig. 5B). On day 5, the collagen deposition area of H-STR group was nearly twice that of control group, and L-STR group was not significantly increased compared with that of control group (Fig. 5F). The staining results showed that STR treatment effectively reduced inflammatory cell infiltration, promoted angiogenesis, cell proliferation, and enhanced collagen deposition.

3.3. Immunofluorescence analysis of CD31 and PCNA

Compared with the control group, the L-STR group exhibited a slight increase in CD31 and PCNA expression. In contrast, both the rb-bfgf group and H-STR group showed significantly higher levels of CD31 and PCNA expression than the control group at both 5 days and 8 days (Fig. 6A and B). On 5 days, the expression of CD31 in H-STR group was twice that in control group while the expression of PCNA in H-STR group was three times that in control group (Fig. 6C and D). These findings indicated that angiogenesis and cell proliferation were upregulated in all drug group, especially in H-STR group and rb-bfgf group. Thus, our results provided that STR may play an important role in promoting angiogenesis and cell proliferation.

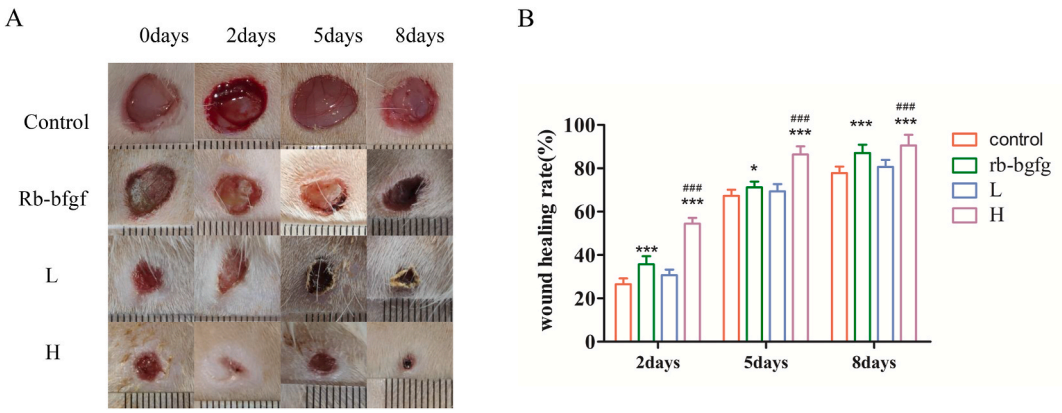

Fig. 4. The effects of STR on skin wound healing by topical treatment. (A) Wound pictures were captured after treatment for 0, 2, 5, 8 days. (B) Wound healing rate was analyzed. (*$p < 0.05$ and **$p < 0.01$ *vs* control group, $^{\#}p < 0.05$ and $^{\#\#}p < 0.01$ vs L group).

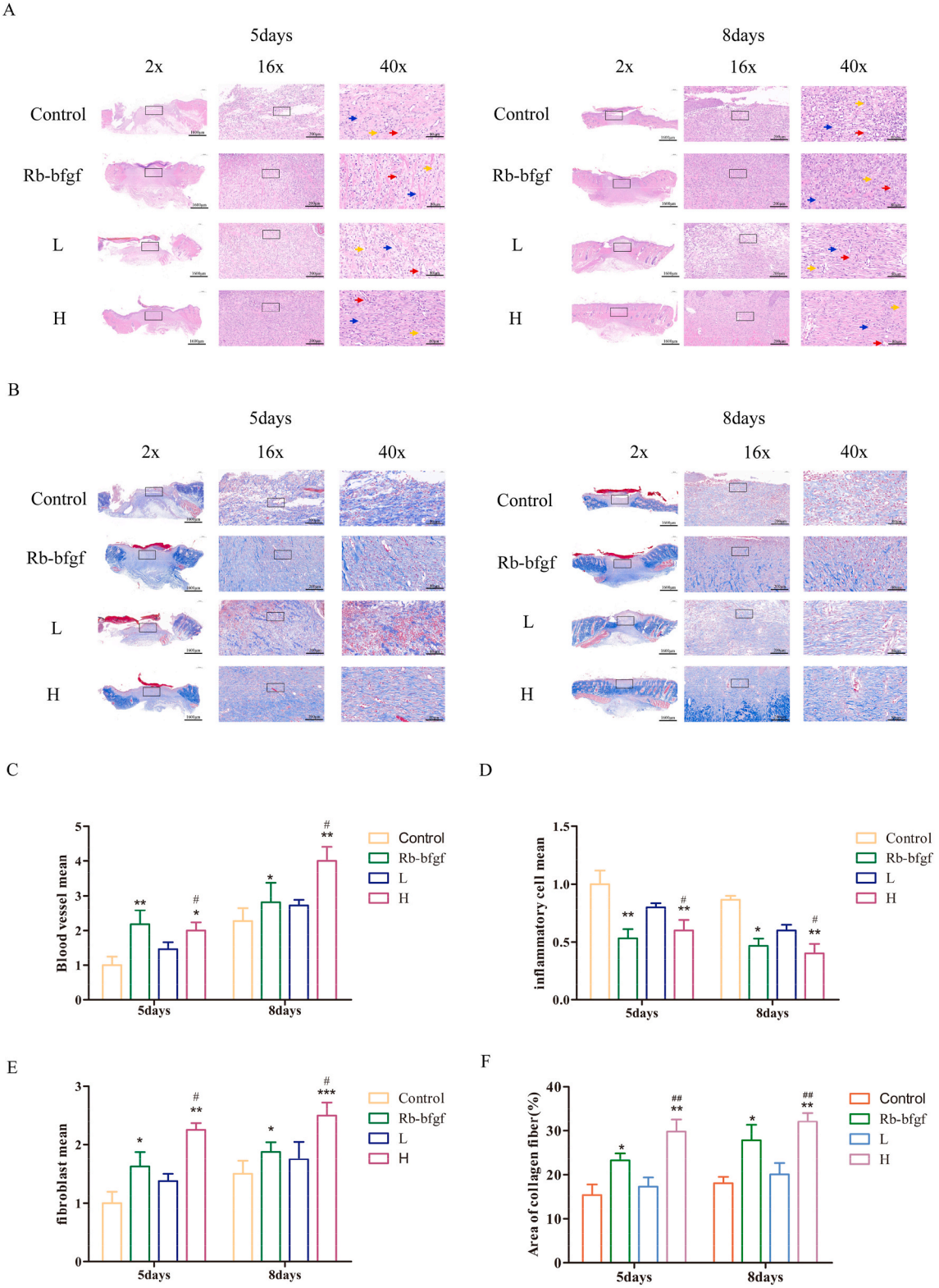

Fig. 5. Representative Histopathological staining of skin after trauma in different groups. (A) H&E staining images of 5days and 8days; (B) Masson staining images of 5 days and 8 days; (C) The mean of inflammatory cells; (D) The mean of vessels; (E) The mean of fibroblasts; (F) The area of collagen deposition (*$p < 0.05$ and **$p < 0.01$ *vs* control group, $^{\#}p < 0.05$ and $^{\#\#}p < 0.01$ vs L group).

3.4. STR and wound healing-related gene analysis

A total of 52 STR-related genes were screened using the criteria probability >0 and a total of 5009 wound healing-related genes were screened using Score >0. The intersection of STR-related genes and wound healing-related genes yielded 35 genes, accounting for 67 % of STR-related genes (Table 1 and Fig. 7A). The protein interaction network diagram showed the relationships between the targets. The more lines the target connected, the more important the target was to the network (Fig. 7B). A total of 23 targets had high intermediate centrality (Table 2) and the number of edges was 57 (Fig. 7C).

3.5. Hub node enrichment analysis

The GO enrichment analysis of hub nodes identified 447 enriched GO terms ($P < 0.05$), including 116 biological processes, 36 molecular functions, and 29 cellular components. The top 10 GO terms were shown in Fig. 8A. Ninety-three pathways were obtained

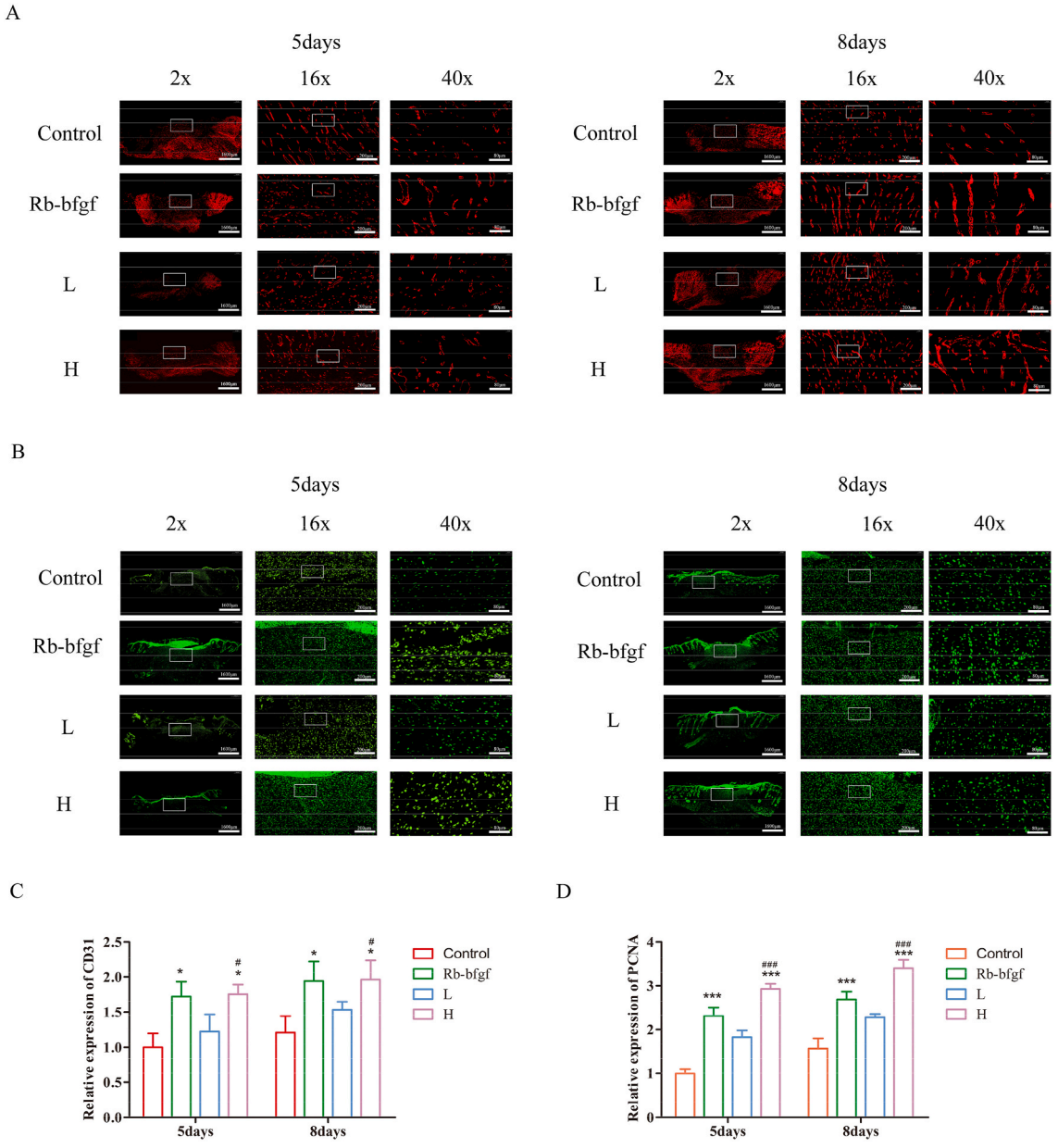

Fig. 6. Immunofluorescence of skin after trauma in different groups. (A) Immunofluorescence of CD31 at 5days and 8days; (B) Immunofluorescence of PCNA at 5days and 8days; (C) The expression of CD31; (D) The expression of PCNA (*$p < 0.05$ and **$p < 0.01$ *vs* control group, $^{\#}p < 0.05$ and $^{\#\#}p < 0.01$ vs L group).

Table 1
The intersection of STR-related genes and wound healing-related genes.

Potential targets	Gene name	Uniprot ID
Adenosine A1 receptor (by homology)	ADORA1	P30542
Adenosine A2a receptor (by homology)	ADORA2A	P29274
Adenosine A2b receptor	ADORA2B	P29275
Serine/threonine-protein kinase B-raf	BRAF	P15056
Carbonic anhydrase IX	CA9	Q16790
Cyclin-dependent cyclin E	CCNE1	P24864
Cyclin-dependent cyclin E	CCNE2	O96020
Cyclin-dependent kinase 1	CDK1	P06493
Cyclin-dependent kinase 2	CDK2	P24941
Eukaryotic initiation factor 4A-I	EIF4A1	P60842
Coagulation factor VII/tissue factor	F3	P13726
78 kDa glucose-regulated protein	HSPA5	P11021
Heat shock cognate 71 kDa protein	HSPA8	P11142
Integrin alpha-4	ITGA4	P13612
Integrin beta-1	ITGB1	P05556
Integrin beta-7	ITGB7	P26010
Tyrosine-protein kinase JAK2	JAK2	O60674
Galectin-1	LGALS1	P09382
Galectin-3	LGALS3	P17931
Dual specificity mitogen-activated protein kinase kinase 1	MAP2K1	Q02750
MAP kinase ERK2	MAPK1	P28482
MAP kinase p38 alpha	MAPK14	Q16539
Hepatocyte growth factor receptor	MET	P08581
Matrix metalloproteinase 13	MMP1	P4545
Matrix metalloproteinase 2	MMP2	P08253
Matrix metalloproteinase 8	MMP8	P22894
Matrix metalloproteinase 9	MMP9	P14780
Nerve growth factor receptor Trk-A	NTRK1	P04629
Purinergic receptor P2Y12 (by homology)	P2RY12	Q9H244
Peptidyl-prolylcis-trans isomerase NIMA-interacting 1	PIN1	Q13526
Sodium channel protein type IX alpha subunit	SCN9A	Q15858
NAD-dependent deacetylasesirtuin 2	SIRT2	Q8IXJ6
Glucose transporter (by homology)	SLC2A1	P11166
Tyrosine-protein kinase SYK	SYK	P43405
DNA topoisomerase I	TOP1	P11387

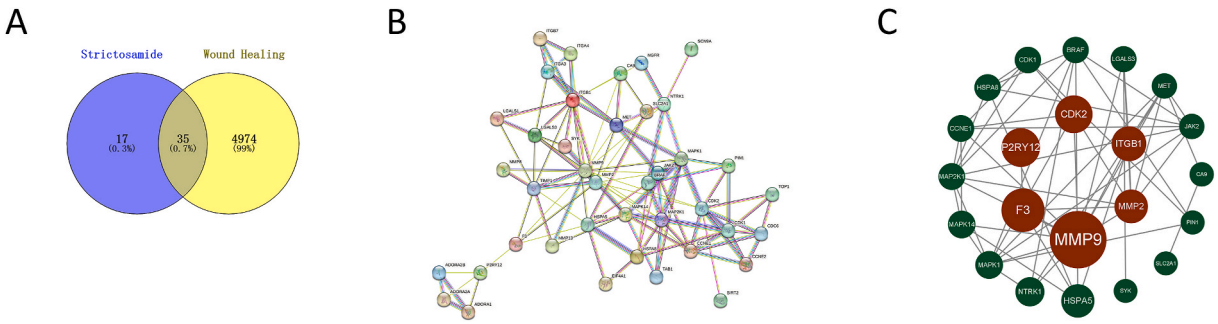

Fig. 7. Screening of STR and wound healing hub genes. (A). Venn diagram of the STR and the wound healing-related targets; (B). PPI network of STR and wound healing intersected genes; (C). PPI network of STR and wound healing.

from the KEGG enrichment analysis ($P < 0.05$), and the main signaling pathways were pathways in cancer, PI3K-AKT signaling pathway and hepatitis B (Fig. 8B). The PI3K/AKT pathway regulates inflammation, growth, and apoptosis. Therefore, PI3K/AKT was closely related to pathways in cancer [30]. So we believed that PI3K/AKT was the most promising target for STR treatment of wound healing.

3.6. Compound-target-pathway-disease network

The compound-target-pathway-disease network of STR for treating wound healing was shown in Fig. 9. Fifteen signaling pathways associated with wound healing function were screened through gene set enrichment analysis. Accordingly, we hypothesized that the therapeutic effect of STR on wound healing primarily involves the modulation of NTRK1, ITGB1, MAP2K1, SYK, ITGA4, CCNE1, CDK2, MAPK1, JAK2 and MET targets to mediate the PI3K/AKT signaling pathway. Based on the above prediction results, we decided to

Table 2
STR and wound healing hub genes.

Gene name	Betweenness
MMP9	414.30823
F3	243.92728
P2RY12	186
CDK2	173.87749
ITGB1	138.54437
MMP2	124.86912
HSPA5	120.39055
NTRK1	69.08254
MAPK1	52.435425
MAPK14	50.141705
MAP2K1	39.743435
CCNE1	38.927418
HSPA8	37.465366
CDK1	35.822365
BRAF	33.98521
LGALS3	29.181313
MET	22.202381
JAK2	22.154978
ITGA4	14.2047615
CA9	9.077778
PIN1	6.1391053
SLC2A1	4.552525
SYK	2.9666667

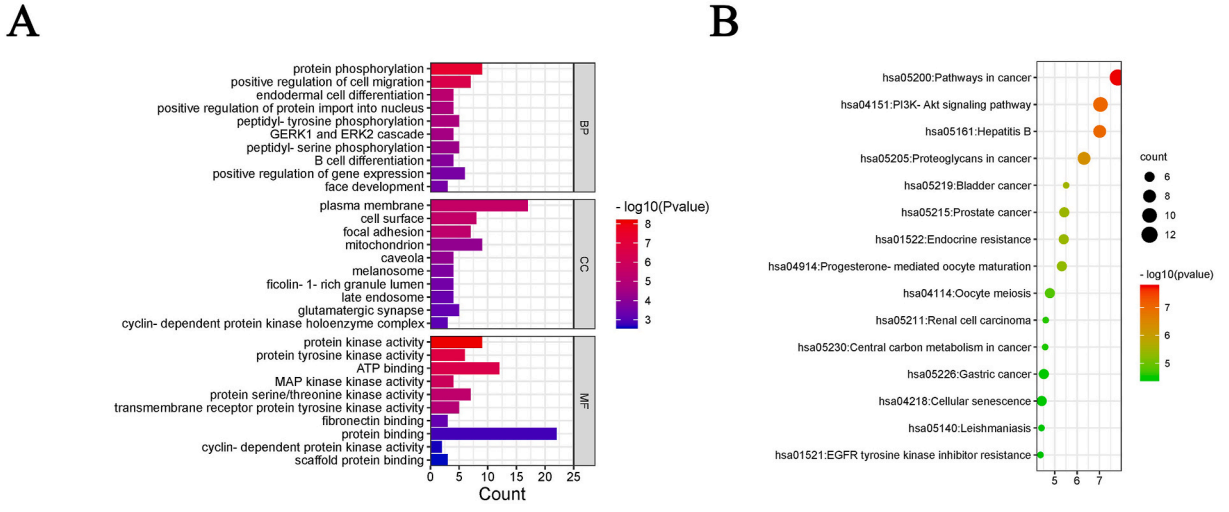

Fig. 8. The analysis of STR and wound healing hub genes. (A). STR and wound healing hub genes GO enrichment analysis; (B). The KEGG pathway enrichment of hub genes.

verify whether STR could promote wound healing by regulating the PI3K/AKT pathway through *in vivo and in vitro* experiments.

3.7. Molecular docking

The molecular docking was performed on the key proteins (AKT and PI3K) within the PI3K/AKT signaling pathways. The lower the binding energy, the higher the affinity between the receptor and the ligand, maybe result in the higher the possibility of their interaction. When the binding energy was <0, the ligand and the receptor could bind freely. The binding sites of STR with PI3K and AKT protein were shown in Fig. 10, and the binding energies were −13.37 and −7.58 kcal/mol (Table 3). The interaction between the ligand and the receptor mainly included carbon–hydrogen bond, conventional hydrogen bond, and van der Waals, among others, wherein the conventional hydrogen bond acted as the main factor for the formation of protein–drug complexes.

As shown in Fig. 10, STR bonded with ARG849, ARG690, GLU880, ASP788 and TYR787 of PI3K (Fig. 10A) through five hydrogen and bonds with ASP292 and ASP274 of AKT by two hydrogen (Fig. 10B). These results further validated the relationship between STR and these proteins, thereby supporting the results obtained from network pharmacology.

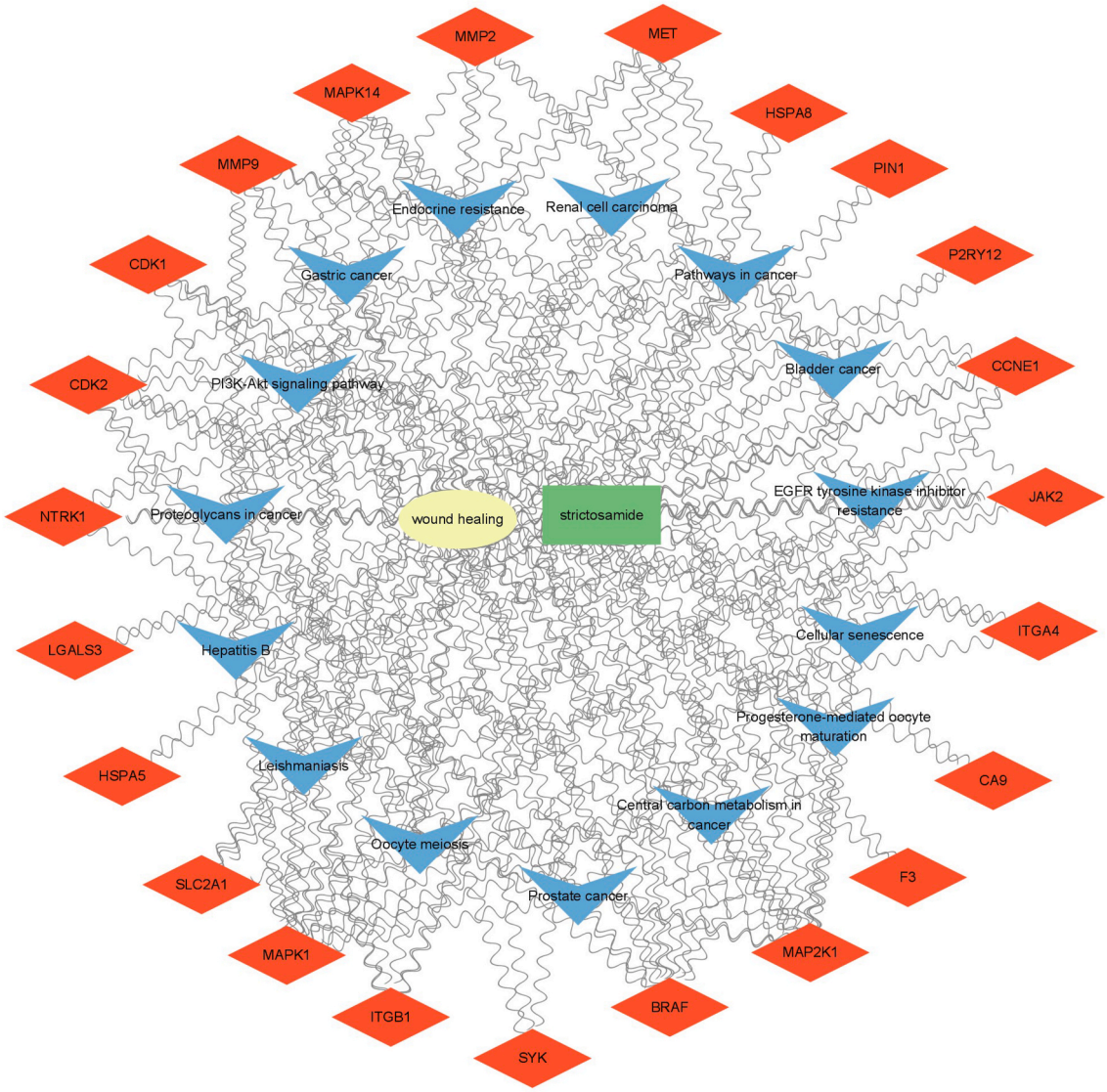

Fig. 9. The compound-target-pathway-disease network of STR for treating wound healing: yellow circle represents STR, red diamond represent targets, blue triangle represent signaling pathways, and green rectangle represent wound healing.

3.8. STR regulated the PI3K/AKT signaling pathway in vivo and vitro

The mTOR pathway regulates cell growth and metabolism, and researchers usually studied both the PI3K/AKT pathway and the mTOR pathway during wound healing [31]. Based on the pathway prediction results, we determined the expression levels and phosphorylation of PI3K, AKT, and mTOR. As shown in Fig. 11A, B, 11C and 11D, the application of STR led to increased phosphorylations of PI3K, AKT and mTOR in both H-STR group and rb-bfgf group compare to the control group. These findings suggested that STR could accelerate wound healing through activation of the PI3K/AKT pathway.

In addition, the effects of different STR concentrations on the proliferation of L929 cells and HUVEC cells were measured within 24 h. As shown in Fig. 12A and B, when STR concentration varied in the range of 0, 20, 40, 80, 160, 320, 625 and 1250 μM, the proliferation ability of L929 cells and HUVEC cells was significantly enhanced. The highest L929 cell survival rate was 157.44 ± 1.36 % at 40 μM. Similarly, the highest HUVEC cell survival rate was 139.12 ± 9.27 % at 80 μM. These results showed that STR could promote cell proliferation while also STR could up-regulate phosphorylation of PI3K, AKT and mTOR *in vitro*. The most significant increase in phosphorylation was observed at a concentration of 40 μM (Fig. 13A, B, 13C and 13D).

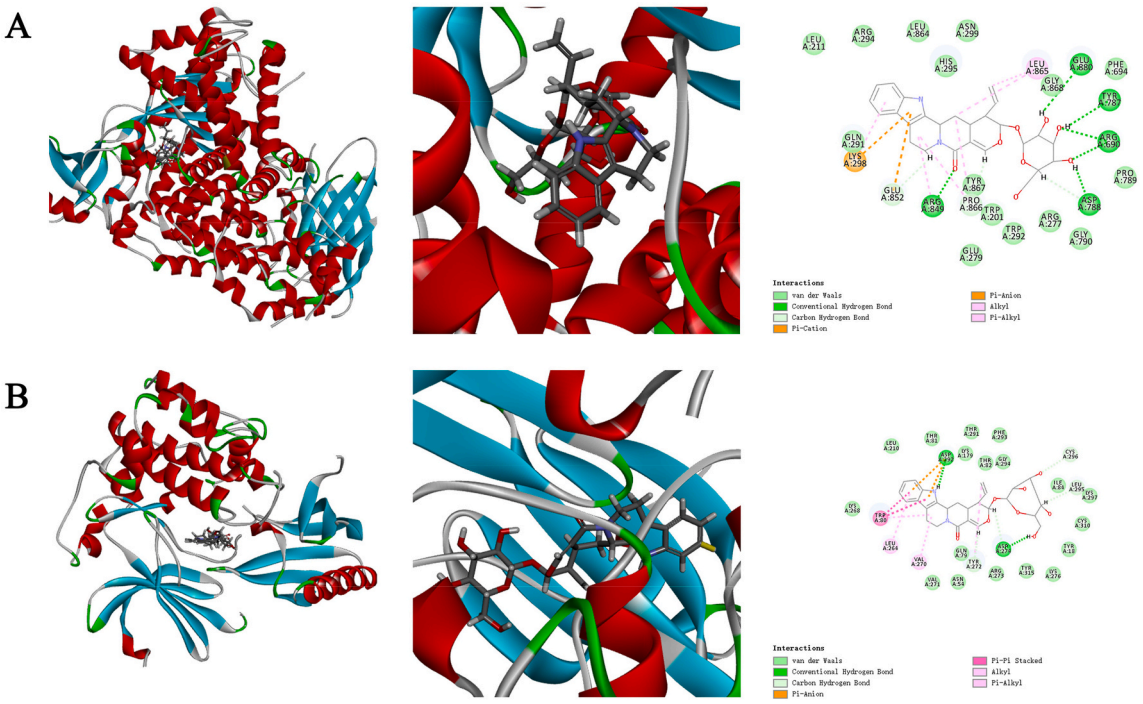

Fig. 10. The binding mode of STR with PI3K and AKT; (A). STR with PI3K; (B). STR with AKT.

Table 3
The binding energy of strictosamide with PI3K and AKT.

Component	Target	PDB ID	Blind Energy (kcal/mol)
Strictosamide	PI3K	6HHI	−13.37
	AKT	6AUD	−7.58

4. Discussion

STR was a compound with a higher content and had good pharmacological activity in *Nauclea* genus [32]. Previous studies had demonstrated its bioavailability of intravenous and oral injection was 95 % and 10.44 %, respectively [33,34]. And STR could treat gastric ulcers by reducing inflammation and protecting cell from damage [26]. These findings provided foundation for investigating the therapeutic potential of STR in wound healing.

After skin injury, exposed endothelial cells, collagen, and tissue factors could activate the platelet aggregation, leading to platelet degranulation and the release of chemokines and growth factors to form clots, all of which successfully stop bleeding [35]. Neutrophils were the first cells to migrate to the site of injury, clearing away debris and bacteria while creating a favorable environment for wound healing [36]. Macrophages secrete pro-inflammatory factors that, together with neutrophils, increase the inflammatory response [37]. However, a prolonged inflammatory response could hinder wound healing [38]. Moreover the macrophages could promote neutrophil apoptosis through endocytosis and reduce inflammation [39]. Ke's study demonstrated that a novel dressing effectively promoted wound healing through the modulation of inflammatory cells and promotion of anti-inflammatory factors [40]. Previous studies have reported that STR inhibits ear edema and reduces the number of white blood cells in the abdominal cavity of mice [41]. The findings of our study closely align with these results. After the analysis of image J software, the H&E staining results showed that STR did have the effect of reducing inflammatory cells. However, the expression levels of the pro-inflammatory factors IL-1β, IL-6 and TNF-α, as well as the anti-inflammatory factors IL-4, IL-10 and TGF-β need further study.

Inflammation played an important role in wound healing. However, GO analysis indicated that STR could influence cell proliferation. Blood vessels serve as conduits for nutrient delivery throughout the body, ensuring adequate nourishment for tissue and organ regeneration [4]. M2 macrophages and micro vascular endothelial cells could secrete VEGF, and VEGF could promote the proliferation of vascular endothelial cells [42]. CD31 was a marker of vascular endothelial cells. The previous studies had demonstrated an up-regulation of CD31 expression during the process of wound healing [43]. Our immunofluorescence results demonstrated that STR significantly up-regulated the expression of CD31, suggesting a potential role for STR in promoting angiogenesis by enhancing vascular endothelial cell formation. The L-STR group, however, did not exhibit a significant promoting effect. This may be attributed to the possibility that the concentration of STR does not reach the effective range. In the proliferative stage, both the blood vessels formed

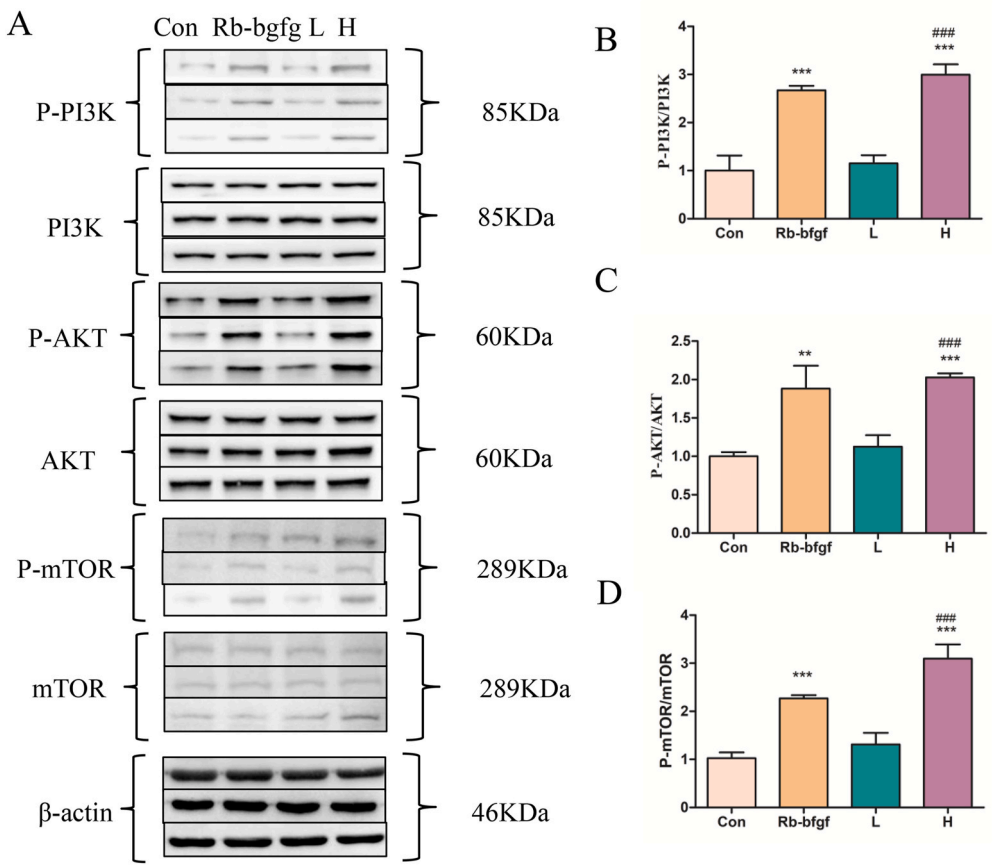

Fig. 11. The protein expressions of AKT, P-AKT, PI3K, P-PI3K, mTOR, P-mTOR and β-action in tissue by Western blot. (A) was the protein expressions of AKT, P-AKT, PI3K, P-PI3K, mTOR, P-mTOR and β-action by Western blot. (B–D) were the relative expression of protein ($^{*}p < 0.05$ and $^{**}p < 0.01$ *vs* control group, $^{\#}p < 0.05$ and $^{\#\#}p < 0.01$ vs L group).

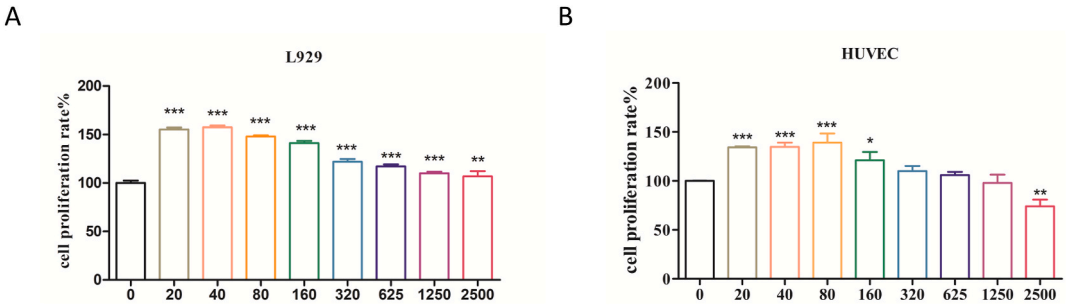

Fig. 12. (A) CCK-8 assay for the effect of different concentrations of STR on the activity of L929 cells in culture for 24 h ($^{*}p < 0.05$ and $^{**}p < 0.01$ *vs* control group), (B) CCK-8 assay for the effect of different concentrations of STR on the activity of HUVEC cells in culture for 24 h ($^{*}p < 0.05$ and $^{**}p < 0.01$ *vs* control group).

rapidly and cells proliferated rapidly [44]. At the same time, macrophages could promote the proliferation and migration of epithelial cells and fibroblasts, and accelerate wound healing [45]. Chen et al. had demonstrated that PCNA serves as a crucial marker for cell proliferation through immunofluorescence [46]. In our study, the increased expression of PCNA indicated that STR could promote cell proliferation. The rapid proliferation and migration of fibroblasts could form a protective film over the wound, reducing the risk of infection [47]. Fibroblasts also secreted a large number of collagen fibers and matrix components to provide support for angiogenesis [48]. Collagen deposition in each group was visualized through Masson staining, revealing that STR could promote collagen deposition.

In this study, the mechanism of STR treating wound healing was speculated through a network pharmacology, molecule docking

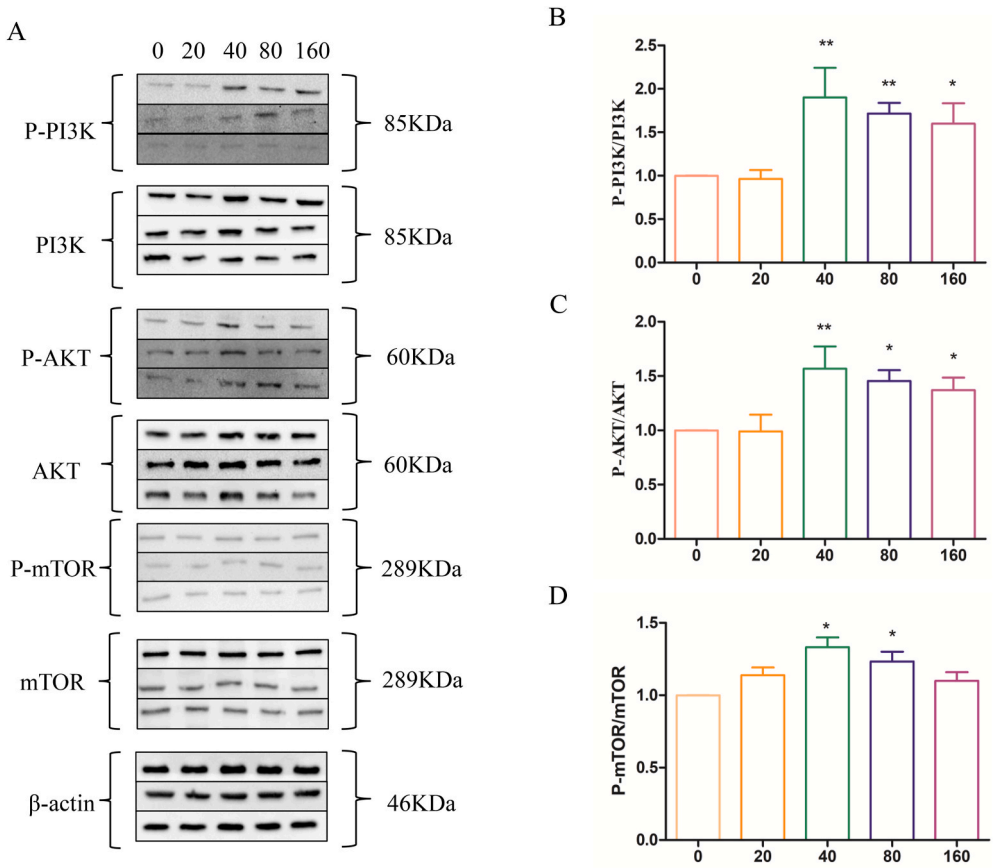

Fig. 13. The protein expressions of AKT, P-AKT, PI3K, P-PI3K, mTOR, P-mTOR and β-action in L929 cell by Western blot. (A) was the protein expressions of AKT, P-AKT, PI3K, P-PI3K, mTOR, P-mTOR and β-action by Western blot. (B–D) were the relative expression of protein (*$p < 0.05$ and **$p < 0.01$ *vs* control group, $^{\#}p < 0.05$ and $^{\#\#}p < 0.01$ vs L group).

and experimental validation. Twenty-three potential targets closely associated with wound healing and STR were identified. Enrichment analysis of the constructed STR-target-pathway network suggested that the wound healing mechanism of STR may involve in PI3K/AKT pathway by acting NTRK1, ITGB1, MAP2K1, MAPK1, ITGB7, JAK2, MET targets. The PI3K/AKT signaling pathway was widely involved in wound healing, which coincides with our network pharmacology prediction.

PI3K could be activated by growth factors, such as VEGF [48]. AKT was one of the client proteins of PI3K. Then, P-AKT could regulate the protein level of phosphorylated mTOR, thereby regulating replication in cell proliferation and differentiation. It had important implications for wound healing [49]. Previous studies had shown that regulation of protein phosphorylation in the PI3K/AKT pathway could promote mTOR phosphorylation and subsequently promote cell proliferation, migration and angiogenesis [39,50,51]. Our study showed that STR increased the expression level of P-PI3K, P-AKT and P-mTOR. This finding suggested that STR may promote WH through activation of the PI3K/AKT signaling pathway.

The GO analysis with a network pharmacology-based approach indicated that STR may repair wound by participating in the cell response to phosphorylation of protein, positively regulates cell migration and endothelial cell differentiation during wound healing processes. Our results had showed that STR up-regulated the phosphorylation of PI3K and AKT. Interestingly, the PI3K/AKT pathway was closely associated to cell proliferation and differentiation [52].

Endothelial cells could undergo differentiation and have remarkable plasticity. During embryonic development, different types of cells, such as hematopoietic stem cells, heart valve progenitor cells, and even cardiac fibroblasts and smooth muscle cells, were produced from specialized endothelial cells [53]. Our results demonstrated that the expression of CD31and PCNA was significantly increased in the STR treatment group. This indicates that STR treatment group could promote vascular endothelial cell differentiation.

The KEGG enrichment analysis indicated that PI3K/AKT signaling may be the mechanism of STR in wound healing. Interestingly, our results suggested that STR could significantly enhance the phosphorylation of PI3K and AKT. It indicated that STR could promote wound healing through the PI3K/AKT pathway.

This study showed that STR had a potential therapeutic effect on wound healing. The advantage of STR was obvious. On the eighth day after the wound formed, the wound was almost healed. Recent studies had reported that many drugs, such as paeoniflorin [54], red ginseng [55] and alternanthera brasiliana [56], take 10 days or more to achieve this effect. Also, as PI3K/AKT involves multiple signal pathways, through which signal does STR affect angiogenesis need further study.

5. Conclusion

In this study, the mechanism of STR promoting wound healing was predicted. The animal experiment demonstrated that STR could promote angiogenesis and cell proliferation via the PI3K/AKT signaling pathways (Fig. 14). This study revealed the mechanism of STR promoting wound healing and may provide a new sight for future research on STR activity and wound healing.

Funding

This work was supported by National Natural Science Foundation of China (No. 82160826) and Hainan Provincial Natural Science Foundation of China (No. 2019RC207).

Ethics approval and consent to participate

This study was reviewed and approved by the Animal Ethical Committee of Hainan Medical University, with the approval number: No. HYLL-2022-277.

Consent for publication

Not applicable.

Data availability statement

Data associated with this study has not been deposited into a publicly available repository and the data and materials generated or analyzed during this study were available from the corresponding author on reasonable request.

CRediT authorship contribution statement

Gu-xu Ming: Writing – review & editing, Writing – original draft, Visualization, Validation, Supervision, Software, Project administration, Methodology, Investigation, Formal analysis, Data curation, Conceptualization. **Jun-yan Liu:** Writing – original draft, Software, Project administration, Methodology, Formal analysis, Data curation, Conceptualization. **Yu-huang Wu:** Validation, Methodology, Formal analysis. **Li-yan Li:** Methodology, Data curation. **Xin-yue Ma:** Writing – original draft, Formal analysis. **Pei Liu:**

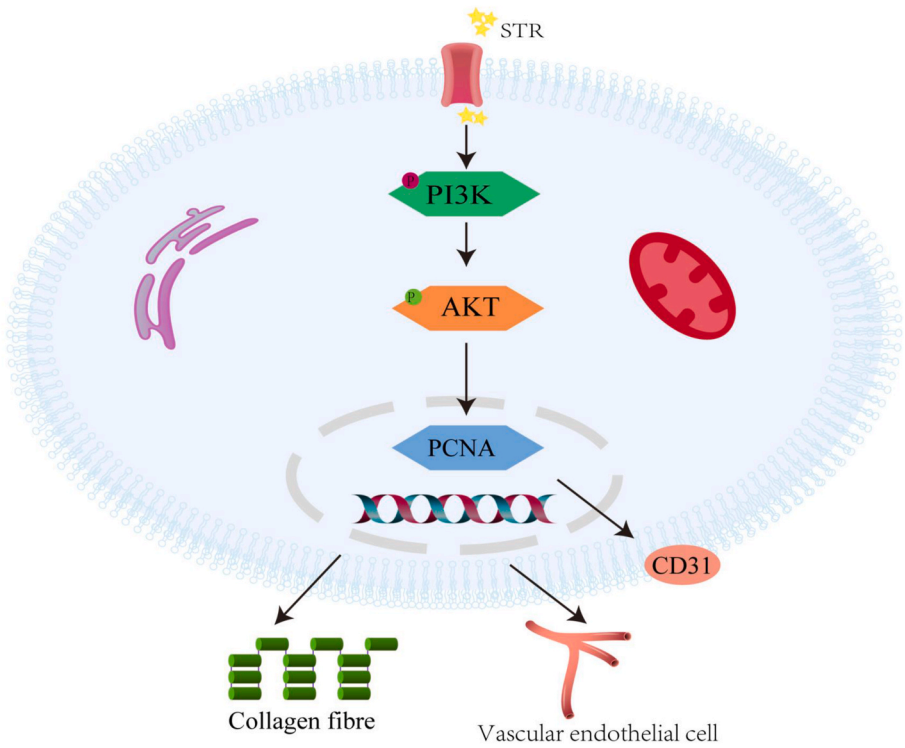

Fig. 14. Molecular mechanism of STR promoting wound healing through PI3K/AKT signaling pathway.

Methodology. **Yi-peng Pan:** Methodology. **Xiao-ning He:** Resources, Funding acquisition. **Yong-hui Li:** Writing – review & editing, Resources, Funding acquisition.

Declaration of competing interest

The authors declare that they have no known competing financial interests or personal relationships that could have appeared to influence the work reported in this paper.

Acknowledgments

Thanks to the Pharmaceutical Analysis Key disciplines of Hainan Medical University for the support of this paper.

Appendix A. Supplementary data

Supplementary data to this article can be found online at https://doi.org/10.1016/j.heliyon.2024.e30169.

References

[1] C.D.d.S. Horinouchi, D.A.G.B. Mendes, B.d.S. Soley, E.F. Pietrovski, V.A. Facundo, A.R.S. Santos, D.A. Cabrini, M.F. Otuki, Combretum leprosum Mart. (Combretaceae): potential as an antiproliferative and anti-inflammatory agent, J. Ethnopharmacol. 145 (2013) 311–319.
[2] T. Michel, E. Destandau, G. Le Floch, M.E. Lucchesi, C. Elfakir, Antimicrobial, antioxidant and phytochemical investigations of sea buckthorn (Hippophaë rhamnoides L.) leaf, stem, root and seed, Food Chem. 131 (2012) 754–760.
[3] S. Barrientos, H. Brem, O. Stojadinovic, M. Tomic-Canic, Clinical application of growth factors and cytokines in wound healing, Wound Repair Regen. 22 (2014) 569–578.
[4] T.J. Shaw, P. Martin, Wound repair at a glance, J. Cell Sci. 122 (2009) 3209–3213.
[5] D.T. Nguyen, D.P. Orgill, G.F. Murphy, The Pathophysiologic Basis for Wound Healing and Cutaneous Regeneration, 2009, pp. 25–57.
[6] Y. Mi, L. Zhong, S. Lu, P. Hu, Y. Pan, X. Ma, B. Yan, Z. Wei, G. Yang, Quercetin promotes cutaneous wound healing in mice through Wnt/β-catenin signaling pathway, J. Ethnopharmacol. 290 (2022) 115066.
[7] G. Caligiuri, Mechanotransduction, immunoregulation, and metabolic functions of CD31 in cardiovascular pathophysiology, Cardiovasc. Res. 115 (2019) 1425–1434.
[8] W. Strzalka, A. Ziemienowicz, Proliferating cell nuclear antigen (PCNA): a key factor in DNA replication and cell cycle regulation, Ann. Bot. 107 (2011) 1127–1140.
[9] J.E. Celis, R. Bravo, P.M. Larsen, S.J. Fey, CYCLIN: a nuclear protein whose level correlates directly with the proliferative state of normal as well as transformed cells, Leuk. Res. 8 (1984) 143–157.
[10] H.C. Zhang, H.Y. Sun, G.Y. Sun, Y.C. Chao, J.Y. Sun, Research progress on pharmacological activity of Dalbergia L, Shanxi Med. J. 45 (21) (2016) 2496–2498 (in·Chinese).
[11] B. Liu, Q. Geng, Z. Cao, L. Li, P. Lu, L. Lin, L. Yan, C. Lu, Nauclea officinalis: a Chinese medicinal herb with phytochemical, biological, and pharmacological effects, Chin. Med. 17 (2022) 141.
[12] Y. Wang, J.H. Liao, L.X. Sun, Review of Nauclea officinalis and its preparations, Asia-Pac. Tradit. Med. 14 (8) (2018) 80–84.
[13] W. Li, D.L. Zhu, G.H. Li, L. Li, X.J. Zou, Q. Li, Clinical observation of treatment of cystic acne by combination of traditional Chinese and Western medicine, Hebei Med. J. 37 (23) (2015) 3605–3607 (in·Chinese).
[14] G. Wang, H. Wang, H. Liu, Y. Wang, Z. Lin, L. Sun, The rapid profiling and simultaneous determination of 12 major alkaloids in Nauclea officinalis by UPLC-Q-TOF-MS and HPLC-ESI-MS/MS, Anal. Methods 13 (2021) 5787–5803.
[15] C.A.J. Erdelmeier, A.D. Wright, J. Orjala, B. Baumgartner, T. Rali, O. Sticher, New indole alkaloid glycosides from Nauclea orientalis, Planta Med. 57 (1991) 149–152.
[16] L. Dhooghe, K. Mesia, E. Kohtala, L. Tona, L. Pieters, A.J. Vlietinck, S. Apers, Development and validation of an HPLC-method for the determination of alkaloids in the stem bark extract of Nauclea pobeguinii, Talanta 76 (2008) 462–468.
[17] S. Khanna, M. Venojarvi, S. Roy, N. Sharma, Dermal wound healing properties of redox-active grape seed proanthocyanidins, Free Radical Biol. Med. 33 (2002) 1089–1096.
[18] D. Li, J. Chen, J. Ye, X. Zhai, J. Song, C. Jiang, J. Wang, H. Zhang, X. Jia, F. Zhu, Anti-inflammatory effect of the six compounds isolated from Nauclea officinalis Pierrc ex Pitard, and molecular mechanism of strictosamide via suppressing the NF-kappaB and MAPK signaling pathway in LPS-induced RAW 264.7 macrophages, J. Ethnopharmacol. 196 (2017) 66–74.
[19] K. Mesia, R.K. Cimanga, L. Dhooghe, P. Cos, S. Apers, J. Totte, G.L. Tona, L. Pieters, A.J. Vlietinck, L. Maes, Antimalarial activity and toxicity evaluation of a quantified Nauclea pobeguinii extract, J. Ethnopharmacol. 131 (2010) 10–16.
[20] S.Y. Mai, Y.H. Li, X.G. Zhang, Y.R. Wang, J.Q. Zhang, A. Jia, A new indole alkaloid with HUVEC proliferation activities from Nauclea officinalis, Nat. Prod. Res. 35 (2021) 3049–3055.
[21] R. Li, X. Ma, Y. Song, Y. Zhang, W. Xiong, L. Li, L. Zhou, Anti-colorectal cancer targets of resveratrol and biological molecular mechanism: analyses of network pharmacology, human and experimental data, J. Cell. Biochem. 120 (2019) 11265–11273.
[22] L.-R. Jiang, Y. Qin, J.-L. Nong, H. An, Network pharmacology analysis of pharmacological mechanisms underlying the anti-type 2 diabetes mellitus effect of guava leaf, Arab. J. Chem. 14 (2021) 103143.
[23] J.W. Tang, X.S. Xiong, C.L. Qian, Q.H. Liu, P.B. Wen, X.Y. Shi, S. Blen Dereje, X. Zhang, L. Wang, Network pharmacological analysis of ethanol extract of Morus alba Linne in the treatment of type 2 diabetes mellitus, Arab. J. Chem. 14 (2021) 103384.
[24] J. Zhang, X. Liu, W. Zhou, G. Cheng, J. Wu, S. Guo, S. Jia, Y. Liu, B. Li, X. Zhang, M. Wang, A bioinformatics investigation into molecular mechanism of Yinzhihuang granules for treating hepatitis B by network pharmacology and molecular docking verification, Sci. Rep. 10 (2020) 11448.
[25] X. Sun, Y. Yang, T. Liu, H. Huang, Y. Kuang, L. Chen, Evaluation of the wound healing potential of Sophora alopecuroides in SD rat's skin, J. Ethnopharmacol. 273 (2021) 113998.
[26] Q. Jia, H. Zhang, Y. Su, X. Liu, J. Bai, W. Lang, Q. Shi, M. Feng, Strictosamide alleviates the inflammation in an acute ulcerative colitis (UC) model, J. Physiol. Biochem. 77 (2021) 283–294.
[27] T.A.M. Andrade, D.S. Masson-Meyers, G.F. Caetano, V.A. Terra, P.P. Ovidio, A.A. Jordão-Júnior, M.A.C. Frade, Skin changes in streptozotocin-induced diabetic rats, Biochem. Biophys. Res. Commun. 490 (2017) 1154–1161.

[28] W.-n. Zhang, Y. Gao, K. Li, J.-b. Chao, X.-m. Qin, A.-p. Li, Exploration into the mechanism of total flavonoids of Astragali Radix in the treatment of nephrotic syndrome based on network pharmacology, Acta Pharm. Sin. (2018) 1429–1441.
[29] X. Yuan, B. Wang, Network pharmacology study on action mechanism of Tripterygium Glycosides Tablets in treatment of nephrotic syndrome, Drugs Clin. 34 (2019) 3209–3214. %@ 1674-5515.
[30] M.R. Khezri, R. Jafari, K. Yousefi, N.M. Zolbanin, The PI3K/AKT signaling pathway in cancer: molecular mechanisms and possible therapeutic interventions, Exp. Mol. Pathol. 127 (2022) 104787.
[31] X. Zou, Q. Yang, Y. Xiao, L. Zhang, H. Xiao, H. Lei, X. Zhang, X. Bai, W. Xiong, Endothelial progenitor-cell-derived exosomes induced by astragaloside IV accelerate type I diabetic-wound healing via the PI3K/AKT/mTOR pathway in rats, Front. Biosci.-Landmark 28 (2023) 282.
[32] N. Li, J. Zhang, Y. Zhang, Z. Ma, J. Liao, H. Cao, M. Wu, Chromatographic fingerprints analysis and determination of seven components in Danmu preparations by HPLC-DAD/QTOF-MS, Chin. Med. 15 (2020) 19.
[33] X. Hu, Y.-F. Lv, K.-S. Bi, LC–MS–MS analysis of strictosamide in rat plasma, and application of the method to a pharmacokinetic study, Chromatographia 69 (2009) 1073–1076.
[34] C. Dai, W. Xiao, Y. Liang, L. Xie, G. Wang, G. Ding, Z. Meng, J. Zhang, T. Guan, A. Kang, X. Zheng, T. Xie, C. Li, Q. Zhao, W. Liu, L. Zhao, J. Xu, Validated liquid chromatography mass spectrometry method for quantitative determination of strictosamide in dog plasma and its application to pharmacokinetic study, Biomed. Chromatogr. 25 (2011) 1338–1342.
[35] G.G. Gauglitz, H.C. Korting, T. Pavicic, T. Ruzicka, M.G. Jeschke, Hypertrophic scarring and keloids: pathomechanisms and current and emerging treatment strategies, Mol. Med. 17 (2011) 113–125.
[36] M. Phillipson, P. Kubes, The healing power of neutrophils, Trends Immunol. 40 (2019) 635–647.
[37] J.P. Cooke, Inflammation and its role in regeneration and repair, Circ. Res. 124 (2019) 1166–1168.
[38] N.X. Landén, D. Li, M. Ståhle, Transition from inflammation to proliferation: a critical step during wound healing, Cell. Mol. Life Sci. 73 (2016) 3861–3885.
[39] S. Khanna, S. Biswas, Y.L. Shang, E. Collard, A. Azad, C. Kauh, V. Bhasker, G.M. Gordillo, C.K. Sen, S. Roy, Macrophage dysfunction impairs resolution of inflammation in the wounds of diabetic mice, PLoS One 5 (3) (2010) e9539.
[40] Q. Ke, X. Zhang, Y. Yang, Q. Chen, J. Su, Y. Tang, L. Fang, Wearable magnetoelectric stimulation for chronic wound healing by electrospun CoFe2O4@CTAB/PVDF dressings, ACS Appl. Mater. Interfaces 16 (2024) 9839–9853.
[41] N. Li, L. Cao, Y. Cheng, Z.Q. Meng, Z.H. Tang, W.J. Liu, Z.Z. Wang, G. Ding, W. Xiao, In vivo anti-inflammatory and analgesic activities of strictosamide from Nauclea officinalis, Pharmaceut. Biol. 52 (2014) 1445–1450.
[42] L. Lei, G. Wan, X. Geng, J. Sun, Y. Zhang, J. Wang, C. Yang, Z. Pan, The total iridoid glycoside extract of Lamiophlomis rotata Kudo induces M2 macrophage polarization to accelerate wound healing by RAS/p38 MAPK/NF-κB pathway, J. Ethnopharmacol. 307 (2023) 116193.
[43] D. Ghosh, J.R. Yaron, M.R. Abedin, S. Godeshala, S. Kumar, J. Kilbourne, F. Berthiaume, K. Rege, Bioactive nanomaterials kickstart early repair processes and potentiate temporally modulated healing of healthy and diabetic wounds, Biomaterials 306 (2024) 122496.
[44] C. Dunnill, T. Patton, J. Brennan, J. Barrett, M. Dryden, J. Cooke, D. Leaper, N.T. Georgopoulos, Reactive oxygen species (ROS) and wound healing: the functional role of ROS and emerging ROS-modulating technologies for augmentation of the healing process, Int. Wound J. 14 (2017) 89–96.
[45] H. Zhang, X. Nie, X. Shi, J. Zhao, Y. Chen, Q. Yao, C. Sun, J. Yang, Regulatory mechanisms of the Wnt/β-catenin pathway in diabetic cutaneous ulcers, Front. Pharmacol. 9 (2018).
[46] Y.F. Chen, K.J. Wu, L.R. Siao, H.Y. Tsai, Trilinolein, a natural triacylglycerol, protects cerebral ischemia through inhibition of neuronal apoptosis and ameliorates intimal hyperplasia via attenuation of migration and modulation of matrix metalloproteinase-2 and RAS/MEK/ERK signaling pathway in VSMCs, Int. J. Mol. Sci. 23 (2022) 12820.
[47] Z. Zhang, T. Chen, W. Liu, J. Xiong, L. Jiang, M. Liu, Paeonol accelerates skin wound healing by regulating macrophage polarization and inflammation in diabetic rats, KOREAN J. PHYSIOL. PHARMACOL. 27 (2023) 437–448.
[48] M.D. Cui, Z.H. Pan, L.Q. Pan, Danggui buxue extract-loaded liposomes in thermosensitive gel enhance in vivo dermal wound healing via activation of the VEGF/PI3K/Akt and TGF-beta/Smads signaling pathway, Evid. base Compl. Alternative Med. 2017 (2017) 8407249 eCAM.
[49] N. Pazyar, R. Yaghoobi, E. Rafiee, A. Mehrabian, A. Feily, Skin wound healing and phytomedicine: a review, Skin Pharmacol. Physiol. 27 (2014) 303–310.
[50] H. Zhang, S. Chen, X. Yan, M. Zhang, Y. Jiang, Y. Zhou, Egg white-derived peptide KPHAEVVLR promotes wound healing in rat palatal mucosa via PI3K/AKT/mTOR pathway, Peptides 168 (2023) 171074.
[51] F. Shan, L.L. Liang, C. Feng, H.B. Xu, Z.R. Wang, W.L. Liu, LAMC2 regulates proliferation, migration, and invasion mediated by the Pl3K/AKT/mTOR pathway in oral 31 (4) (2023) 481–493.
[52] D.M. Ornitz, N. Itoh, The Fibroblast Growth Factor signaling pathway, Wiley interdisciplinary reviews, Dev. Biol. 4 (2015) 215–266.
[53] E. Dejana, K.K. Hirschi, M. Simons, The molecular basis of endothelial cell plasticity, Nat. Commun. 8 (2017) 14361.
[54] X. Dong, Z. He, G. Xiang, L. Cai, Z. Xu, C. Mao, Y. Feng, Retracted: paeoniflorin promotes angiogenesis and tissue regeneration in a full-thickness cutaneous wound model through the PI3K/AKT pathway, J. Cell. Physiol. 235 (2020) 9933–9945.
[55] K.-S. Park, D.-H. Park, The effect of Korean Red Ginseng on full-thickness skin wound healing in rats, J. Ginseng Res. 43 (2019) 226–235.
[56] R. Marchete, S. Oliveira, L. Bagne, J.I.d.S. Silva, A.P. Valverde, A.A.d. Aro, M.M. Figueira, M. Fronza, T.M. Bressam, V.F.F.d. Goes, F.O.d. Gaspari de Gaspi, G.M. T. dos Santos, T.A.M. Andrade, Anti-inflammatory and antioxidant properties of Alternanthera brasiliana improve cutaneous wound healing in rats, Inflammopharmacology 29 (2021) 1443–1458.